

Dynamic fuel cell model improvement based on macroscopic energy representation

Mohamed Haidoury, Mohammed Rachidi

Modeling, Information Processing and Control Systems (MPICS), National School of Arts and Crafts, Moulay Ismail University, Meknes, Morocco

Article Info

Article history:

Received Apr 14, 2022

Revised May 30, 2022

Accepted Jun 22, 2022

Keywords:

Chemical delay

Dynamic Model

Energetic Macroscopic

Fuel Cell PEM

Multi-physic's modeling

Representation

ABSTRACT

In this paper, a new dynamic model is presented of the proton exchange membrane fuel cell (PEMFC), using energetic macroscopic representation (EMR). This model is developed for electric automotive applications, powered by a hybrid energy storage system (HESS). The PEMFC can be used as a primary source, the supercapacitors (SC) and/or batteries are the secondary sources. The model design enables the optimization of energy use and the reduction of equipment costs, by involving the fuel cell (FC) in the transient regimes. This model takes into consideration dynamic phenomena, such as double layer capacitance, charge transfer, energy losses caused by the propagation fuel and oxidant delay. The new developed model has been tested and validated using BAHIA bench of HELION/AREVA.

This is an open access article under the [CC BY-SA](https://creativecommons.org/licenses/by-sa/4.0/) license.



Corresponding Author:

Mohamed Haidoury

Modeling, Information Processing and Control Systems (MPICS), National School of Arts and Crafts

Moulay Ismail University

Presidency, Marjane 2, BP:298, Meknes, Morocco

Email: haidoury.mohamed@gmail.com

1. INTRODUCTION

In a global context of greenhouse gas emissions reduction, research activities are focused on the development of solutions, aiming at transportation-related pollution reduction. In the electric vehicles (EV) and mobility sector, PEMFCs are one of the promising technological advancements, for the transportation industry future. This technology ensures significant performances related to the EV range, compared to conventional architectures, powered by a hybrid energy storage system (HESS) based on SCs and batteries. PEMFC is an electrochemical device, used to convert dihydrogen and dioxygen to electrical power, water and heat. Due to its dynamic limitations, PEMFCs are activated only in the steady state. Therefore, SCs and/or batteries should be integrated to improve the dynamic performances and extend the PEMFC lifespan. This integration generates very high loads in the secondary sources during the transient regime, characterized by high varying energy demand. In order to ensure an optimal and more efficient contribution of fuel cell (FC) during transient regimes, the analysis and control of its dynamic response represents a key issue. Thus, several works have focused on the dynamic modeling of different energy sources, particularly FCs. These models take into consideration the phenomena that occur in transient regimes, such as: double layer capacitance, geometric capacitance and energy losses related to the system [1]-[3].

In this context, a simplified mathematical model of the proton exchange membrane fuel cell (PEMFC) has been developed, based on the variation of pressure, temperature and flow rate of hydrogen and air, such as the MATLAB/Simulink blocks models [4], [5]. Thus, a previous study was proposed by using the simplified mathematical model [6], [7], these works introduce other dynamic mechanisms, such as double

layer and thermal response phenomena. On the other hand, a model based on a simple approach, implementing a second order fuel cell transfer function is also developed in [8]. Moreover, a various studies have been conducted, aiming at the development of a neural network-based model, in order to predict the evolution of PEMFC performance [9]-[12].

Another dynamics models have been proposed, for example the works conducted on dynamic models of proton exchange membrane fuel cell (PEMFC), using electrical circuits [13]-[15]. Similarly, a research team [16], [17], have been particularly interested in the FC's energetic modeling, using the bond graph (BG) approach. The BG's model has been evaluated using modelica software platform. On the other hand, a model of a PEMFC has been developed using the energetic macroscopic representation (EMR) approach. This work aimed at local control design, based on the EMR inversion-based rules, in order to control the FC's electrical parameters [18]-[20].

This paper aims at the design of the PEMFC dynamic model, taking into consideration the chemical delay, introduced by propagation of fuel and oxidant. This work allows the construction of the FC local control, which integrates a chemical delay estimator. The evaluation of the developed model was carried out by comparing the developed model and the experimental results, obtained by BAHIA experimental platform. The rest of the paper is structured as follows: The second section will focus on the design of the PEMFC dynamic model using EMR approach. The third section is dedicated to the implementation of the FC local control. The last section presents the experimental results of the developed model.

2. DYNAMIC MODEL AND LOCAL CONTROL

2.1. PEMFC modeling

First, a dynamic model has been developed, taking into consideration several phenomena. It's designed using the EMR approach, based on causal graph principles. The developed PEMFC model is based on the works results of [19], [21], to which a chemical delay model has been developed and integrated, in order to improve the FC model behavior. This phenomenon is introduced by the propagation of fuel and oxidant [22]. The delay that appears during the transient regime, generates a voltage V_r described in (1). Therefore, the implementation of the voltage V_r in the Nernst equation, as shown in Figure 1, allows to improve the FC model.

$$V_r = \lambda_e I_e \cdot \frac{\tau e \cdot s}{\tau e \cdot s + 1} \tag{1}$$

With:

- V_r : Voltage of chemical delay (V);
- λ_e : Constant factor (Ω) ;
- τe : Global flow delay ($\tau e = 80s$).

In the other hand, the collected equations, shown in Figure 1, describe the phenomena by domain, allowing the identification of the PEMFC subsystems and their interactions. Thus, the EMR model can be deduced.

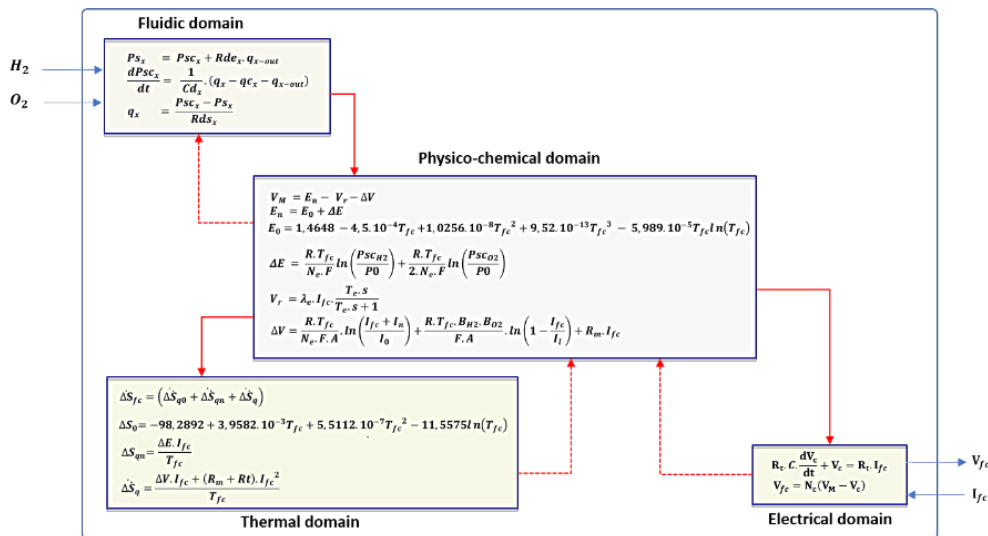


Figure 1. Studied domains and multi-physic equations of PEMFC system

The EMR approach allows to establish the description and organization of multi-physical subsystems, based on the energy conservation principle, the different EMR blocks are collected and explained in Figure 2. Thus, the collected mathematical models illustrated in Figure 1, are reformulated respecting the causality rules. Therefore, the PEMFC EMR model illustrated in Figure 3, implements three types of blocks:

- Source blocks: include the hydrogen source tank, ambient air, and oxygen. The cooling system and the load electrical sub-system;
- Transformation blocks: in this case, the included transformation blocks describe the oxygen and hydrogen line losses;
- Coupling blocks: allow multi/mono-physical coupling, i.e., fluidic, physical-chemical, thermal and electrical domain;
- Accumulation block: includes the double layer capacitance, the geometric capacitance caused by the accumulation of the fluidic lines, and the chemical delay, induced by the propagation of oxygen and hydrogen, as shown in Figure 3.

Source element (energy source)	Mono-physical conversion (without energy storage)	Accumulation element (energy storage)	Coupling element (energy distribution)	Multi-physical conversion (without energy storage)
Estimator block	Control block with a controller (close-loop)	Inversion of coupling element	Control block without controller	Strategy level

Figure 2. Different blocs of EMR

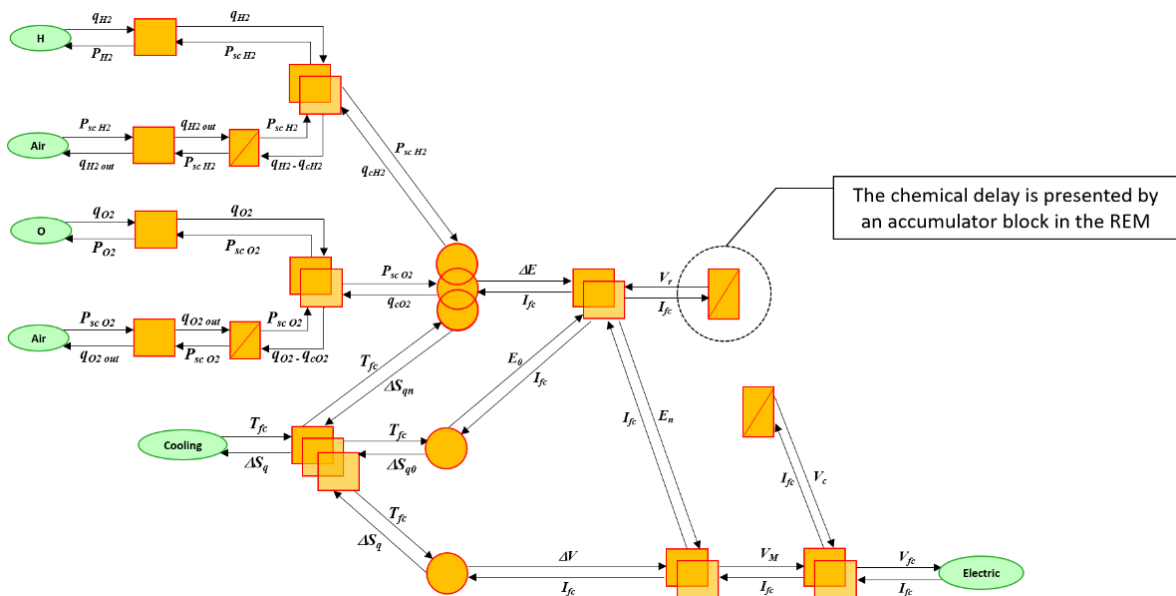


Figure 3. EMR model of PEMFC

2.2. PEMFC local control

The objective of the local control is to ensure a system response able to track the reference, represented by input parameters, such as the input gas flows $Q_{O_2_ref}$, $Q_{H_2_ref}$ and the system temperature T_{fc_ref} to regulate the output voltage V_{fc_ref} . Thus, the control layer is established using system's EMR model inversion, which allows to deduce the tuning and control chains shown in Figure 4. The adopted approach

leads to the organization of subsystems and the construction of the practical control structure (PCS). On the other hand, the research results obtained by [21], [23], dedicated on FC's modeling and control, are used in this study, in order to establish the local control proposed to the new FC's model. Therefore, the implementation of FC's practical local control, should take into consideration the definition of the required estimators and reference values.

$$V_{fc\ ref} \longrightarrow V_{M\ ref} \longrightarrow E_{n\ ref} \longrightarrow \Delta E_{ref} \longrightarrow P_{scO2\ ref} \longrightarrow P_{scO2\ est} \longrightarrow q_{O2} - q_{cO2\ ref} \longrightarrow q_{O2\ ref}$$

Figure 4. PEMFC control chain

The reference parameters are defined from the equations presented in Figure 1 and illustrated in Table 1. The estimated parameters are calculated from the sensors as shown in Table 2. The closed-loop control uses a PI controller C_{PI} shown in (2), designed to satisfy the setpoint input represented by the oxygen flow demand to reach the required load voltage. In the proposed structure, the delay modeled in the model design section, is taken into account and estimated by the load current sensor. The Figure 5 represents the designed PCS based on the FC's EMR.

$$(q_{O2} - q_{cO2})_{ref} = C_{PI}(P_{scO2\ ref} - P_{scO2\ est}) + q_{O2-out_mes} \tag{2}$$

Table 1. PCS's references parameters

References parameters
$V_{M_ref} = \frac{V_{fc_ref}}{Nc} - V_{c_est}$
$V_{n_ref} = V_{M_ref} + \Delta V_{est}$
$\Delta E_{ref} = V_{n_ref} - E_{0_est} + V_{r_est}$
$P_{scO2_ref} = P_0 \cdot \exp\left(\frac{\Delta E_{ref} - \frac{R \cdot T_{mes}}{N \cdot F} \cdot \ln\left(\frac{P_{sch2_est}}{P_0}\right)}{\frac{R \cdot T_{mes}}{2 \cdot N \cdot F}}\right)$
$q_{O2_ref} = q_{O2} - q_{cO2_ref} - q_{cO2_est}$

Table 2. PCS's estimator's parameters

Estimator's parameters
$V_{c_est} = \frac{R_t}{R_t \cdot C \cdot s + 1} \cdot I_{mes}$
$\Delta V_{est} = \frac{R \cdot T_{mes}}{N_e \cdot F \cdot A} \cdot \ln\left(\frac{I_{mes} + I_n}{I_0}\right) + \frac{R \cdot T_{mes} \cdot B_{H2} \cdot B_{O2}}{F \cdot A} \cdot \ln\left(1 - \frac{I_{mes}}{I_1}\right) + R_m \cdot I_{mes}$
$V_{r_est} = \lambda_e \cdot I_{mes} \cdot \frac{T_e \cdot s}{T_e \cdot s + 1}$
$E_{0_est} = a + b \cdot T_{mes} + c \cdot T_{mes}^2 + d \cdot T_{mes}^3 + e \cdot T_{mes} \cdot \ln(T_{mes})$
$P_{sch2_est} = P_0 + Rds_{H2} \cdot q_{H2_mes}$
$P_{scO2_est} = P_0 - Rde_{O2} \cdot q_{O2_mes}$
$q_{cO2_est} = \frac{I_{mes}}{2 \cdot N_e \cdot F} \cdot \frac{R \cdot T_{mes}}{P_{scO2_est}}$

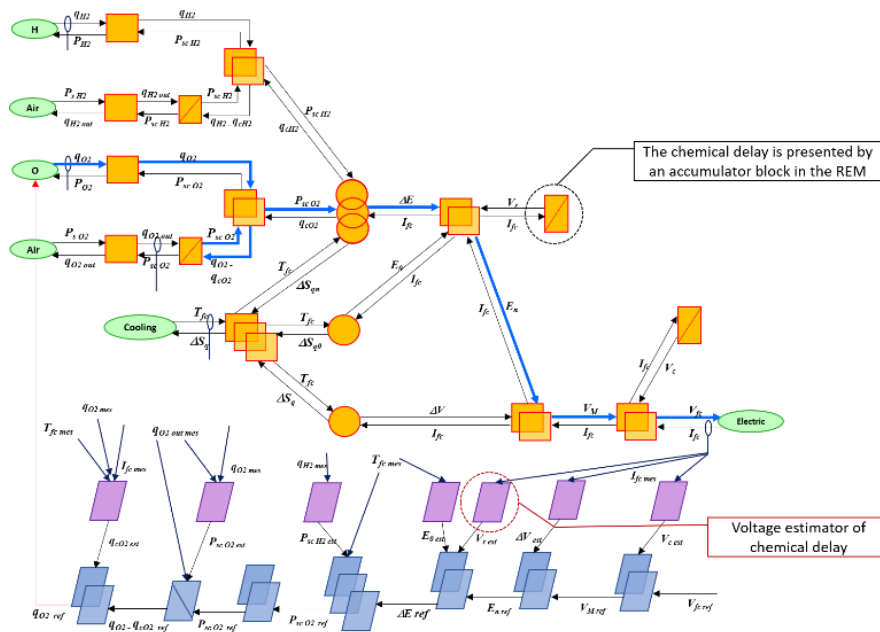


Figure 5. PCS of the PEMFC

4. MATERIAL AND METHODS

In order to evaluate the developed model, the experimental tests have been conducted on BAHIA bench platform as is shown in Figure 6(a). This platform is equipped with 24 PEM cells with a maximum power of 1.2 kW. The output voltage ranging is 13 to 27 V and nominal current is 65 A, operating in hydrogen/air mode [24]. The research works have been achieved on recent experimentation tests. The experimental platform includes three circuits:

- The first circuit is used to assure the hydrogen supply, stored in a pressure tank;
- The second circuit is dedicated to the oxygen supply, which is extracted from air by a controlled fan. The air is pumped through a membrane humidifier before being injected into FC block;
- The third circuit is the cooling circuit, it uses water to decrease the heat of exothermic reactions, and uses a controller to keep the circuit regulated at a reference value of 75 °C.

The BAHIA bench is controlled through a human machine interface (HMI) shown in Figure 6(b), allowing the user to introduce a power or current load profile, to set the oxygen stichometry coefficient ranging from 1.5 to 2.5 and the operating temperature. The measurements of the system's sensors are recorded in real time by an acquisition module (gas flows and pressures, temperature, voltage, current and power). The collected measurements are then recorded in a file in order to be processed and compared with the developed model response.

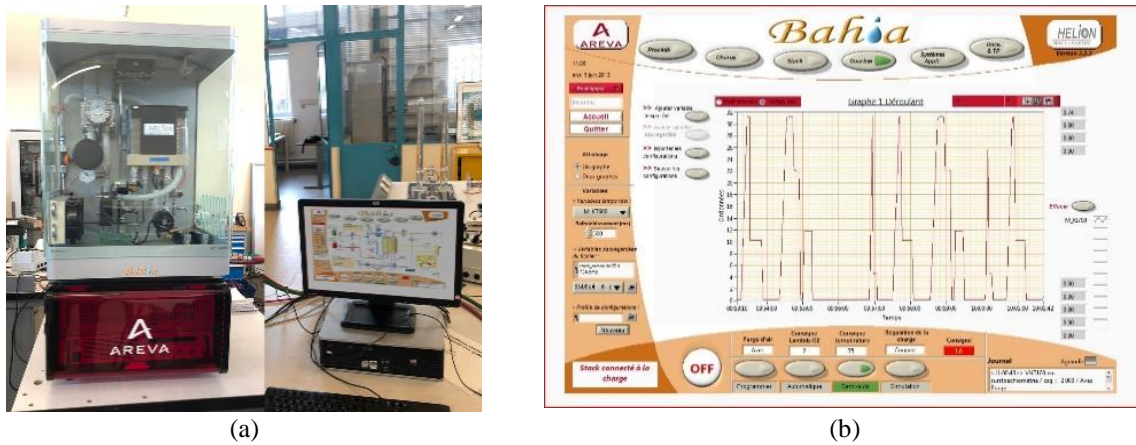


Figure 6. Bahia bench (a) platform PEMFC and (b) human machine interface

The validation of the proposed model should be performed using the load required power profile, in order to evaluate its performances. The used power supply is designed for an EV, it's calculated from urban driving cycle (ECE-15) and mechanical parameters of the EV in (3) [25] shown in Figure 7. The EV's characteristics are listed in Table 3. The power profile is scaled to 1 kW in order to be adjusted to the bench's maximum power supply. Therefore, the results measured on the BAHIA bench, and collected from the data acquisition module, are compared with the developed model results. The schematic diagram of the experiments is presented in Figure 8.

$$P_m = V(M \cdot g \cdot \sin \alpha + C_r \cdot M \cdot g \cdot \cos \alpha + \frac{M \cdot dV}{dt} + \frac{1}{2} \rho \cdot S \cdot C_x \cdot V^2) \tag{3}$$

Table 3. The different variables in (3)

Variable	Designation	Value
V	Vehicle speed (m/s)	ECE-15 cycle
α	Road Grade (rad)	0 rad
C_r	Coefficient of rolling resistance	0.10
C_x	Aerodynamic coefficient	0.30
g	Gravitational constant (m/s ²)	9.81 m/s ²
ρ	Air density (Kg/m ³)	1.255 Kg/m ³
M	Vehicle mass (Kg)	100 Kg
S	Front surface m ²	2.5 m ²

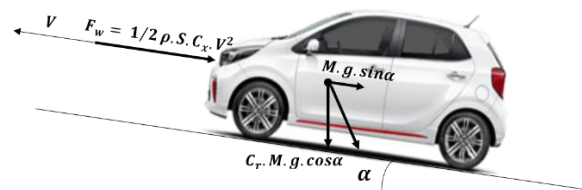


Figure 7. Schematic of resistance forces acting on moving vehicle

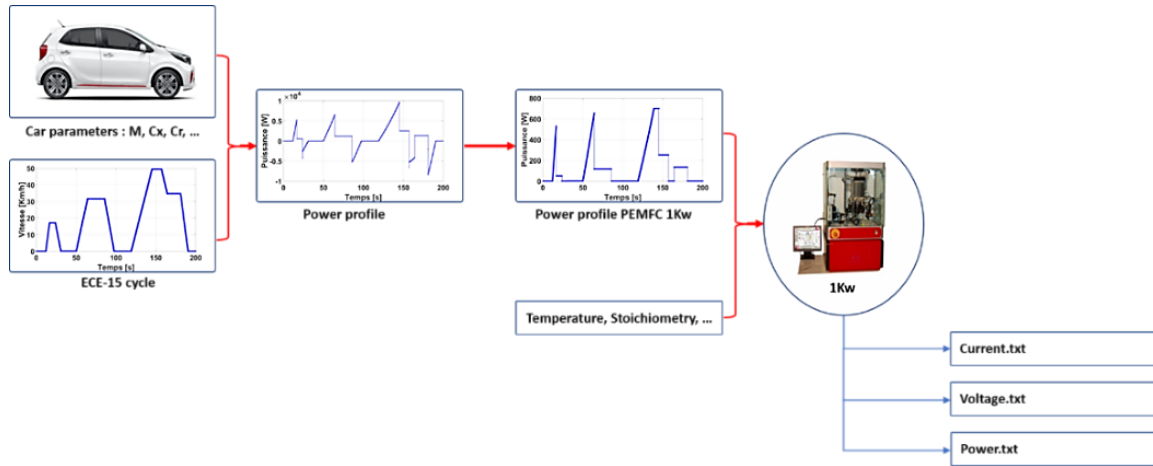


Figure 8. Power profile used in experimentations

5. RESULTS AND DISCUSSIONS

In this section, the dynamic behavior of the developed model is evaluated, comparing its results with those of the BAHIA bench experimental platform. The simulation model was built under MATLAB/SIMULINK environment, using the EMR library, developed at the University of Lille, France. The new PEMFC model and the local control are presented in Figure 9. In addition, the implemented load, is a controlled current source block, based on a programmed behavior similar to one used for the experimentation. The model parameter values used in this simulation are listed in Table 4.

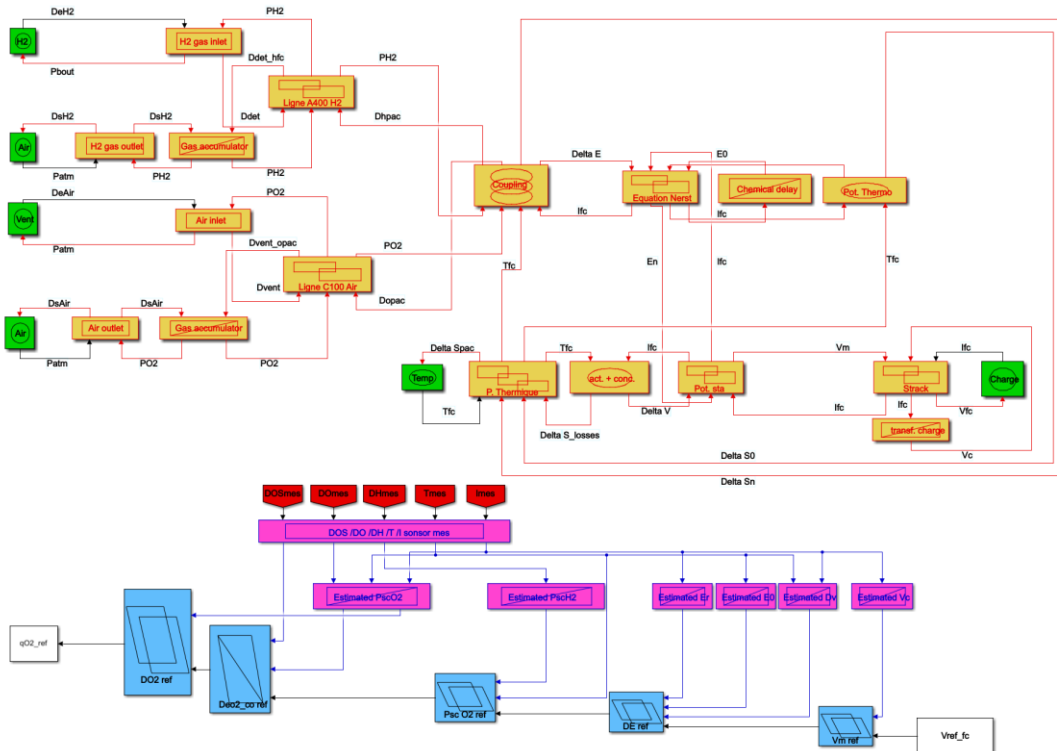


Figure 9. PEMFC simulation model with local control under MATLAB/SIMULINK

The model responses are generated for a stoichiometry value of $C_{stoe_O2}=2$ and temperature $T_{fc}=75$ °C. The curves shown in Figure 10, represent the responses of the developed model, for values defined by an empirical method of the constant factor λe , ranging from 0 to 0.0060. Thus, according to the results obtained, $\lambda e=0.004$ is the value that allows to have a response approximating the response obtained

from the experimental bench BAHIA. In addition, according to recent research works, aiming the same experiments objectives, the value determined by Bahia bench, is of the same scale as the Avista Labs SR-12 500 -W with $\lambda_e=0.00333 \Omega$ [22] and PEMFC PC3F40 cells with $\lambda_e=0.00694 \Omega$ [26]. The constant factor value of $\lambda_e=0.004 \Omega$ is adopted in the developed model.

Table 4. The different variables of the model

Symbol	Variables	Value	Symbol	Variables	Value
F	Faraday constant	96485 C/mol	R_m	Ohmic resistance	$0.9 \cdot 10^{-3} \Omega$
R	Perfect gas constant	8.31446 J/mol/K	R_t	Charge Transfer Resistance	$0.4 \cdot 10^{-3} \Omega$
P_0	Atmospheric pressure	101325 Pa	R_{deH}	Inlet ohmic resistance for the anode	$1.3 \cdot 10^9 \text{ N.s/m}^5$
T_0	Standard temperature	298.15 K	R_{dsH}	Outlet ohmic resistance for the anode	$1.5 \cdot 10^8 \text{ N.s/m}^5$
N_e	Number of electrons exchanged	2	C_{dH}	Fluidic capacity of the anode	$4.56 \cdot 10^{-10} \text{ m}^5/\text{N}$
N_c	Number of stacks	24	R_{deO}	Inlet ohmic resistance for the cathode	$0.4 \cdot 10^9 \text{ N.s/m}^5$
S_a	Active Surface Area	100 cm ²	R_{dsO}	Outlet ohmic resistance for the cathode	$1.5 \cdot 10^8 \text{ N.s/m}^5$
I_n	Internal current	0.1 A	C_{dO}	Fluidic capacity of the cathode	$5.52 \cdot 10^{-10} \text{ m}^5/\text{N}$
I_0	Exchange current	$4.78 \cdot 10^{-6} \text{ A}$	q_{H_2}	Hydrogen inlet flow	$2 \cdot 10^{-4} \text{ m}^3/\text{s}$
I_l	Limiting current	150 A	q_{O_2}	Air inlet flow	$5 \cdot 10^{-4} \text{ m}^3/\text{s}$
I_c	Operating current	80 A	λ_e	Constant factor in calculating Ed	0.0040Ω
A	Charge transfer coefficient	0.6	τ_e	Constant time delay	80s

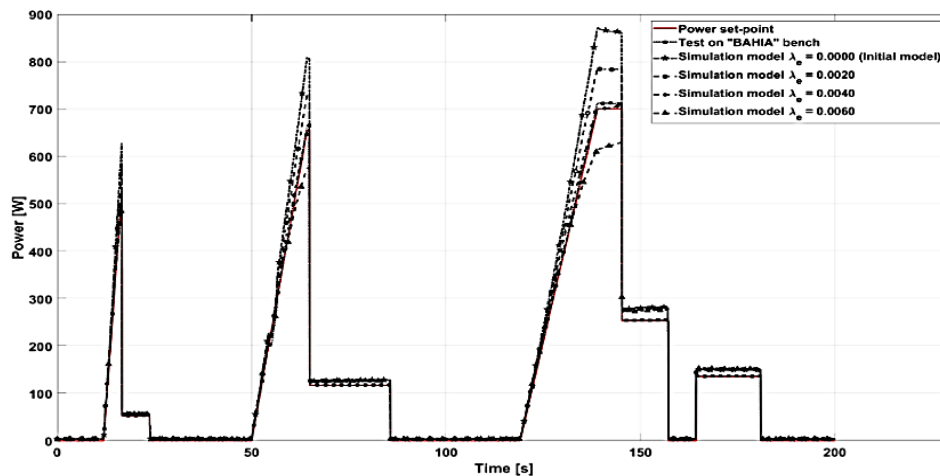
Figure 10. The model responses with constant factor values λ_e

Figure 11 represents the comparison of the steady state characteristics of the proposed model, and the response of BAHIA bench. These characteristics were calculated using a current reference ramp function from 0 to 60 A. The polarization curves comparison, caused by double-layer capacitance effect and the undershoot phenomenon, demonstrates that the developed model agrees well with the experimental results during stationary regimes.

The results shown in Figure 12, represent the PEMFC output voltage of the model and the experimental data, collected from Bahia bench. According to the profiles analysis, the resulting mean square error (MSE) of the model PEMFC output voltage, and calculated power profile, of the ECE 15 cycle is $0.274 \cdot 10^{-3}$, the error found is smaller than that found in [20], which is 0.1463 shown in Figure 13. The comparison between the experimental data and the model developed, show that the results agree well during the transient and stationary regimes.

The validation of the proposed model was also carried out by comparing the power curves of the proposed model and the BAHIA bench. According to Figure 14, both curves are in good agreement and have the same behaviour. The developed model allowed to concretize the effectiveness of the EMR approach, allowing to organize the mathematical models of the studied system, and the determination of the control parameters for H₂ and O₂ sources. This technique combined with the described methodology in this work, gave rise to a simulation platform that can be parameterized under MATLAB/SIMULINK. This simulator is characterized by a dynamic's performances, which provide the possibility of its use in several domains, and improvement paths that can be adopted. In this case, the coupling of the PEMFC model with other sources such as the Battery and/or SC, constituting the (HESS). This solution allows to improve the performances of the main source represented by PEMFC.

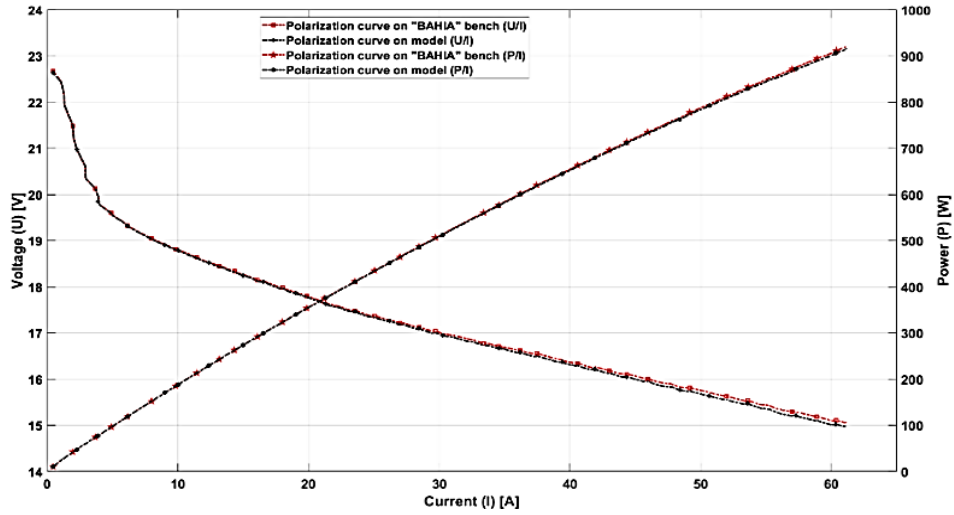


Figure 11. The characteristics of the model and BAHIA bench

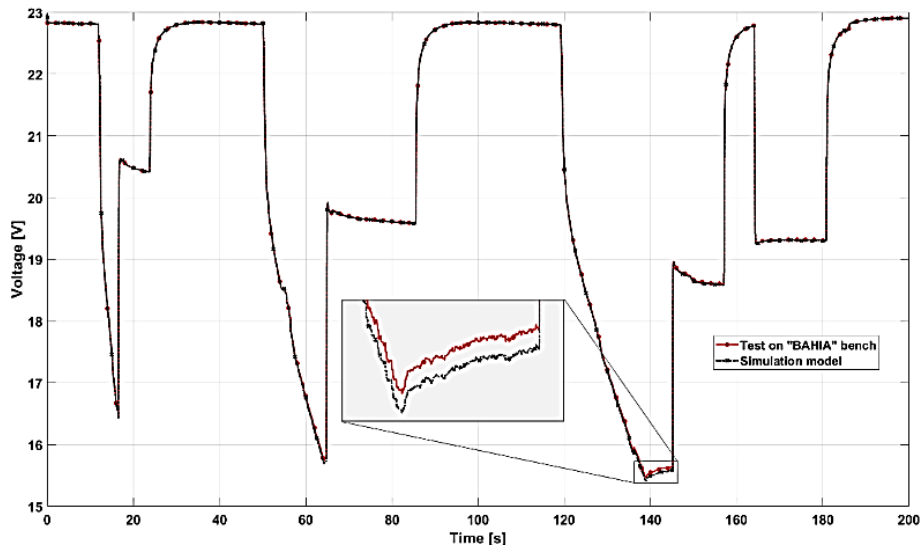


Figure 12. PEMFC response voltage to the ECE-15 cycle

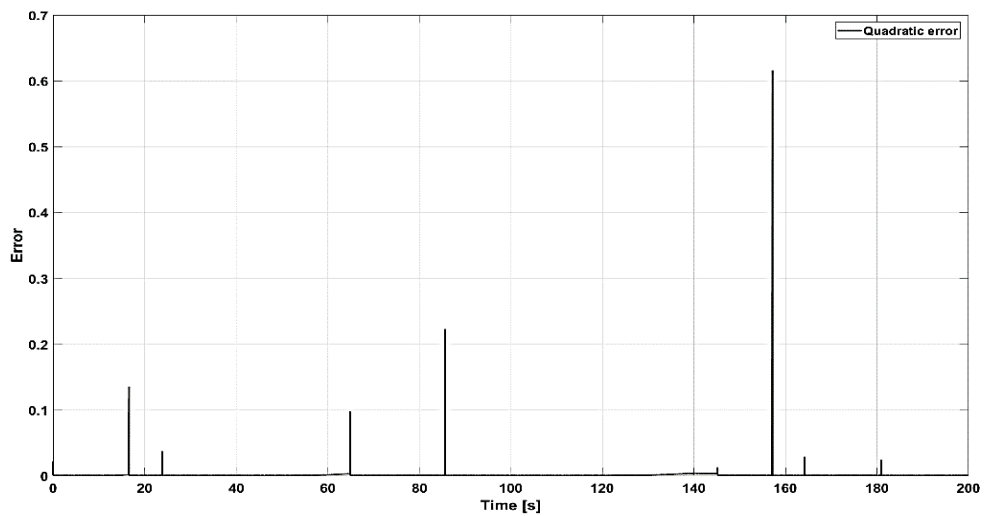


Figure 13. Quadratic error of response to the ECE-15 cycle

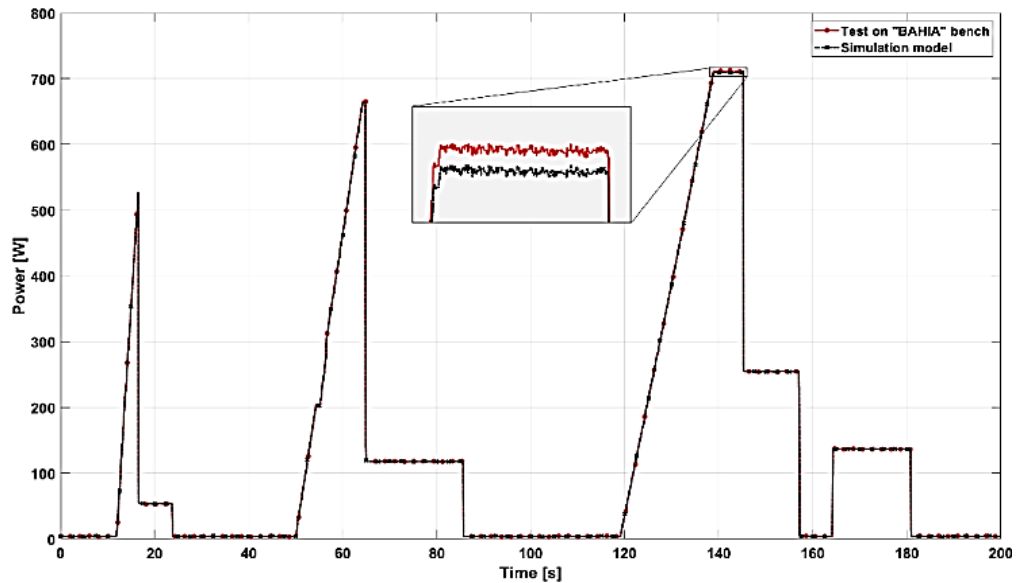


Figure14. PEMFC power response to the ECE-15 cycle

6. CONCLUSION

The dynamic model proposed in this work, is in perfect agreement with the dynamic approaches of the FC developed using EMR. The developed model takes into consideration dynamic phenomena which affect its behaviour, such as fluidic interactions related to fuel flow in hydraulic circuits, the double layer and the charge transfer resulting from the reaction, and the voltage losses caused by electrochemical reactions in a cell. Furthermore, this study also integrates the local control of FC system, by using the practical inverse control. The developed model has been implemented and simulated in MATLAB/SIMULINK environment. Besides, various simulations carried out on the upgraded model, in order to validate the parameterizable simulation model on the BAHIA training bench, which allows to identify and characterize the control parameters of the FC system. The results show that the new developed model is more accurate and provides an excellent performance for EV design.

Finally, the objective of this work has been focused on the modeling, simulation and validation of the PEMFC, which represents the main source of a HESS. Future work will focus on the design, validation and construction of SC and PEMFC-based HESS designed to power an EV, and the design of an energy management strategy ensuring the efficient and optimal supply management provided by the HESS dual-source.




REFERENCES

- [1] J. Jiao, F. Chen, Y. Yu, J. He, and X. Chen, "Modeling and simulation of PEMFC stack dynamic performance," in *Chinese Automation Congress (CAC)*, 2017, pp. 2871-2876, doi: 10.1109/CAC.2017.8243265.
- [2] A. F. Nasef, H. A. Khattab, R. A. Amer, and G. A. Morsy, "Modeling, Simulation and Experimental Performance Analysis of PEM Fuel Cell," in *Twentieth International Middle East Power Systems Conference (MEPCON)*, 2018, pp. 856-861, doi: 10.1109/MEPCON.2018.8635233.
- [3] N. Benchouia, A. E. Hadjadj, A. Derghal, L. Khochemane, and B. Mahmah, "Modeling and validation of fuel cell PEMFC," *Journal of Renewable Energies*, vol. 16, no. 2, pp. 365-377, 2013, doi: 10.54966/jreen.v16i2.386.
- [4] H. Shekhar Das, C. W. Tan, A. Yatim, and N. D. Bin Muhamad, "Proton Exchange Membrane Fuel Cell Emulator Using PI Controlled Buck Converter," *International Journal of Power Electronics and Drive Systems (IJPEDS)*, vol. 8, no. 1, p. 462, 2017, doi: 10.11591/ijped.v8.i1.pp462-469.
- [5] Z. Abdin, C. J. Webb, and E. MacA. Gray, "PEM fuel cell model and simulation in Matlab-Simulink based on physical parameters," *Energy*, vol. 116, pp. 1131-1144, 2016, doi: 10.1016/j.energy.2016.10.033.
- [6] A. F. Abdul Aziz, A. S. Samosir, K. Kamal, I. Amin and S. Mathavan, "Modeling and analyzing the proton exchange membrane of fuel cell (PEMFC) in Matlab/SIMULINK environment," in *IEEE 14th International Multitopic Conference*, 2011, pp. 238-243, doi: 10.1109/INMIC.2011.6151480.
- [7] M. A. Biberici and M. B. Celik, "Dynamic Modeling and Simulation of a PEM Fuel Cell (PEMFC) during an Automotive Vehicle's Driving Cycle," *Engineering, Technology & Applied Science Research*, vol. 10, no. 3, no. 3, 2020, doi: 10.48084/etasr.3352.
- [8] A. Rezazadeh, A. Askarzadeh, and M. Sedighzadeh, "Adaptive Inverse Control of Proton Exchange Membrane Fuel Cell Using RBF Neural Network," *International Journal of Electrochemical Science*, vol. 6, no. 8 p. 14, 2011.
- [9] K. Belmokhtar, M. L. Doumbia, and K. Agboussou, "PEM Fuel Cell Modelling Using Artificial Neural Networks (ANN),"




- International Journal of Renewable Energy Research*, vol. 4, no. 3, pp. 725-730, 2014.
- [10] A. Kheirandish, F. Motlagh, N. Shafiqabady, and M. Dahari, "Dynamic modelling of PEM fuel cell of power electric bicycle system," *International Journal of Hydrogen Energy*, vol. 41, no. 22, pp. 9585–9594, 2016, doi: 10.1016/j.ijhydene.2016.02.046.
- [11] M. S. Ben Yahia, H. Allagui, A. Bouaicha, and A. Mami, "Fuel Cell Impedance Model Parameters Optimization using a Genetic Algorithm," *International Journal of Electrical and Computer Engineering (IJECE)*, vol. 7, no. 1, pp. 196-205, 2017, doi: 10.11591/ijece.v7i1.pp184-193.
- [12] C. Lin-Kwong-Chon, B. Grondin-Pérez, J.-J. A. Kadjo, C. Damour, and M. Benne, "A review of adaptive neural control applied to proton exchange membrane fuel cell systems," *Annual Reviews in Control*, vol. 47, pp. 133–154, 2019, doi: 10.1016/j.arcontrol.2019.03.009.
- [13] G. Sachdeva, "Modeling and Simulation of Fuel Cell (Choi Model) Based 3-Phase Voltage Source Inverter," *International Journal of Power Electronics and Drive Systems (IJPEDS)*, vol. 1, no. 2, pp. 175-178, 2011.
- [14] M. Azri, N. H. Abu Khanipah, Z. Ibrahim, and N. Abd. Rahim, "Fuel Cell Emulator with MPPT Technique and Boost Converter," *International Journal of Power Electronics and Drive Systems (IJPEDS)*, vol. 8, no. 4, pp. 1852-1862, 2017, doi: 10.11591/ijped.s.v8.i4.pp1852-1862.
- [15] C. L. Sandoval Torres, "Contribution to the control of a hybrid energy source based on fuel cell unit coupled to supercapacitors," Ph.D. dissertation, Arts et Métiers Paris Tech, Aix-en-Provence, 2016.
- [16] R. Saisset, G. Fontes, C. Turpin, and S. Astier, "Bond Graph model of a PEM fuel cell," *Journal of Power Sources*, vol. 156, no. 1, pp. 100-107, 2006, doi: 10.1016/j.jpowsour.2005.08.040.
- [17] A. Vasilyev, J. Andrews, L. M. Jackson, S. J. Dunnett, and B. Davies, "Component-based modelling of PEM fuel cells with bond graphs," *International Journal of Hydrogen Energy*, vol. 42, no. 49, pp. 29406–29421, 2017, doi: 10.1016/j.ijhydene.2017.09.004.
- [18] L. Boulon, K. Agbossou, D. Hissel, P. Sicard, A. Bouscayrol, and M.-C. Péra, "A macroscopic PEM fuel cell model including water phenomena for vehicle simulation," *Renewable Energy*, vol. 46, pp. 81–91, 2012, doi: 10.1016/j.renene.2012.03.009.
- [19] L. Boulon, D. Hissel, A. Bouscayrol, and M.-C. Péra, "From Modeling to Control of a PEM Fuel Cell Using Energetic Macroscopic Representation," *IEEE Trans. Ind. Electronics*, vol. 57, no. 6, pp. 1882–1891, 2010, doi: 10.1109/TIE.2009.2026760.
- [20] G. Lopez Lopez, R. Schacht Rodriguez, V. M. Alvarado, J. F. Gomez-Aguilar, J. E. Mota, and C. Sandoval, "Hybrid PEMFC-supercapacitor system: Modeling and energy management in energetic macroscopic representation," *Applied Energy*, vol. 205, pp. 1478–1494, 2017, doi: 10.1016/j.apenergy.2017.08.063.
- [21] L. Boulon, D. Hissel, A. Bouscayrol, M.-C. Péra, and P. Delarue, "Maximal and Practical Control Structure of a PEM Fuel Cell System Based on Energetic Macroscopic Representation," *Fundamentals and Development of Fuel Cells Conference (FDFC)*, p. 11, Jan. 2009.
- [22] C. Wang, M. H. Nehrir, and S. R. Shaw, "Dynamic Models and Model Validation for PEM Fuel Cells Using Electrical Circuits," *IEEE Trans. On Energy Conversion*, vol. 20, no. 2, pp. 442–451, 2005, doi: 10.1109/TEC.2004.842357.
- [23] D. Hissel *et al.*, "A review on existing modeling methodologies for PEM fuel cell systems," *Fundamentals and Development of Fuel Cells Conference (FDFC)*, p. 30, 2008.
- [24] Helion, Manuel d'utilisation et d'installation banc didactique BAHIA type: BAHIA v2.1-a1, V2.1-A1. 2009.
- [25] T. Azib, "Contribution à l'Etude d'Electro-générateurs à Pile à Combustible Conceptions d'Architectures et de Leurs Commandes," Ph.D. University Paris-Sud XI Faculty of Sciences of Orsay, Paris-Sud France, 2010.
- [26] C. R. Patiño, "PEM fuel cell modeling and converters design for a 48 V DC power bus," Ph.D. Rovira i Virgili Tarragona, España, 2012.

BIOGRAPHIES OF AUTHORS



Mohamed Haidoury    was born in Chefchaouen, Morocco in 1985. He received the engineer's degree in electromechanics from the National School of Arts and Crafts, (ENSAM-Meknes) in 2012. He obtained the master's degree in science and technology, specializing in science and information systems from ENSAM Paris-tech center Aix-en-Provence in French, in 2013. Currently, he is pursuing the PhD with the National School of Arts and Crafts (ENSAM-Meknes), in the laboratory Modeling, Information Processing and Control Systems (MTICS), Meknes, Morocco. His research focuses on the modeling and control of a multi-source system. Application to the traction of electric vehicles. He can be contacted at email: haidoury.mohamed@gmail.com.



Mohammed Rachidi    was born in Boujaad, Morocco. He received the engineer's degree from Mohammadia School of Engineers (EMI-Rabat), Morocco, in 1995 and the Ph.D. degree from National School of Arts and Crafts (ENSAM-Meknes), Moulay Ismail University, Meknes, Morocco, in 2017. His search interested power electronics and control of electrical machines. Since 1997, he has been working at National School of Arts and Crafts (ENSAM-Meknes), Moulay Ismail University, Meknes, Morocco, where he is a Professor in the Department of Electromechanical Engineering. He can be contacted at email: morachidi@yahoo.fr.